Mechanism of magnetic flux trapping on superconducting bulk magnetized by pulsed field using a vortex-type coil

2011 Supercond. Sci. Technol. 24 075015

(http://iopscience.iop.org/0953-2048/24/7/075015)

Supercond. Sci. Technol. **24** (2011) 075015 (7pp) doi:10.1088/0953-2048/24/7/075015

Mechanism of magnetic flux trapping on superconducting bulk magnetized by pulsed field using a vortex-type coil

Hiroyuki Fujishiro, Tomoyuki Naito and Mitsuru Oyama

Faculty of Engineering, Iwate University, 4-3-5 Ueda, Morioka 020-8551, Japan

E-mail: fujishiro@iwate-u.ac.jp

Received 25 January 2011, in final form 28 April 2011
Published 1 June 2011
Online at stacks.iop.org/SUST/24/075015

Abstract
Numerical simulations of trapped field B_z and temperature T have been performed for a cryo-cooled superconducting bulk disc after applying a magnetic pulse using a vortex-type coil. Results of the simulation qualitatively reproduced experimental results reported by Ida *et al* (2004 *Physica* C **412–414** 638). Using the vortex-type coil, the magnetic flux does not intrude into the bulk from the periphery but intrudes from both surfaces of the bulk disc. The temperature rise was less than that obtained when using a conventional solenoid coil. The effect of the trapped field enhancement using a long pulse application is small, which suggests that down-sizing of the condenser bank used for the pulsed field magnetization is possible and that the use of the vortex-type coil is desirable for practical applications.

1. Introduction

As a technique for magnetizing bulk REBaCuO (RE: rare earth element or Y), pulsed field magnetization (PFM) has been investigated intensively for practical applications as a substitute for field-cooled magnetization (FCM) because PFM is an inexpensive and mobile experimental set-up that obviates the use of a superconducting solenoid coil. Using a solenoid copper coil, the trapped field B_z achievable by PFM is nonetheless lower than that achievable by FCM because of the large temperature rise caused by the dynamical motion of the magnetic flux. Several approaches have been undertaken to enhance B_z using a multi-pulse technique, including an iteratively magnetizing pulsed field method with reducing amplitude (IMRA) [1] and a multi-pulse technique with stepwise cooling (MPSC) [2]. Considering our obtained experimental results for the time and spatial dependences of the temperature $T(t, r)$ and local field $B_z(t, r)$, and the trapped field B_z on the surface of cryo-cooled REBaCuO bulk during PFM [3–5], we proposed a new PFM technique designated as modified MPSC (MMPSC) [6] and produced the highest field trap of $B_z = 5.20$ T on a 45 mm GdBaCuO bulk at 30 K [7], which is a record high value by PFM to date.

Ida *et al* proposed a new PFM technique using a vortex-type coil. The coil consists of a couple of copper coils and was developed for the magnetization of the bulks by PFM which were used as pole field magnets in the rotor plate in a synchronous motor [8]. They demonstrated that, using the vortex-type coil, the magnetic flux starts to trap on the bulk centre, even for the lower pulsed field B_{ex}, and that the maximum trapped field was better enhanced than that obtained using the solenoid coil. Recently, a higher magnetic field has been trapped in the superconducting bulk, extending it by as much as 140 mm in diameter using a vortex-type coil [9]. However, the mechanism of the field trap has not been clarified.

Several studies of theoretical simulations for PFM have reported using a solenoid coil [10–12]. Experimental research has remained limited and has shown little progress in exploring the enhancement of the trapped field using PFM. Therefore, we have also constructed the framework of theoretical simulation in the superconducting bulk during PFM using the solenoid coil and have simulated the time and spatial dependence of the local field $B_z(t, r)$ and temperature $T(t, r)$ in the superconducting bulk for a single magnetic pulse application [13], for successive pulsed field application with identical strength (SPA) [14], and for MMPSC [15], all of which reproduced the experimental results qualitatively.

As described in this paper, we simulated the trapped field and temperature rise in the superconducting bulk magnetized by a pulsed field using the vortex-type coil. We examined the mechanism of the field trap using the vortex-type coil

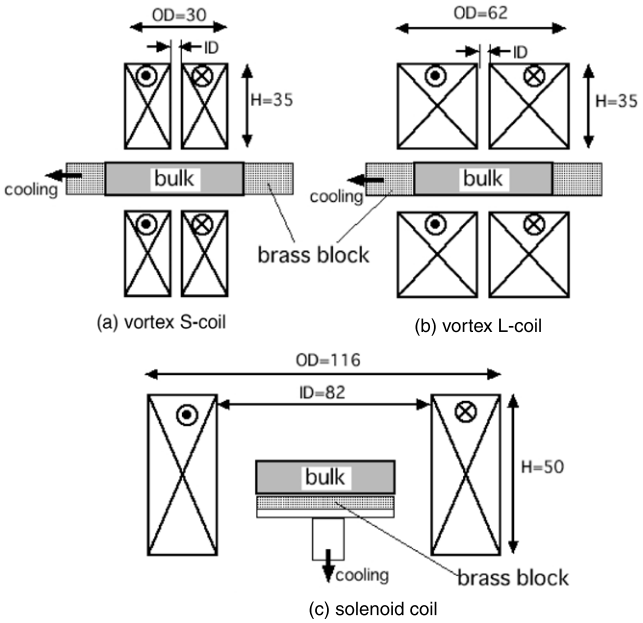

Figure 1. Geometric configuration for the superconducting bulk and the pulsed coil. (a) Vortex S-coil, (b) vortex L-coil, and (c) solenoid coil.

and compared the results with those obtained using the conventional solenoid coil.

2. Theoretical model and simulation

Figure 1 portrays the geometric configuration for the superconducting bulk and the pulsed coil. In the simulation, a set of vortex-type coils was replaced by that of split coils with a small inner dimension. For the vortex-type coil, the bulk (46 mm diameter and 15 mm thickness) was cooled to $T_s = 40$ K from the side surface (along the ab-plane direction) and was placed between a set of vortex-type coils (ID = 4 mm, $H = 35$ mm). In this study, vortex-type coils of two types were examined for the simulation: the vortex S-coil (OD = 30 mm) and the vortex L-coil (OD = 62 mm), as portrayed in figures 1(a) and (b). The distance between the bulk surface and the coil edge was 10 mm. For comparison, the simulation was also performed for the bulk using the solenoid coil (ID = 82 mm, OD = 116 mm, $H = 50$ mm), where the bulk was cooled to $T_s = 40$ K along the c-axis, as presented in figure 1(c). For all cases, the spacing plate of 1 mm in thickness with thermal conductivity, κ_{cont} (=0.5 W m^{-1} K^{-1}), was set between the bulk and the supporting brass block, which imaginarily represented both the cooling power of the refrigerator and the thermal contact of the bulk to the brass block.

Physical phenomena during PFM are described using electromagnetic and thermal equations on the axisymmetric co-ordinate, which were obtained from [12]. Based on the set-up around the bulk, the framework of the theoretical simulation was constructed.

The power-n model ($n = 8$) was used to describe the nonlinear E–J characteristic in the ab-plane of the superconducting bulk as

$$E = E_c \left(\frac{J}{J_c}\right)^n, \tag{1}$$

where J_c is the critical current density in the ab-plane and E_c (=1 × 10^{-6} V m^{-1}) is the reference electric field. The temperature and magnetic field (along the c-axis) dependence of the critical current density $J_c(T, B)$ were described as

$$J_c = \alpha \left\{1 - \left(\frac{T}{T_c}\right)^2\right\}^{\frac{3}{2}} \frac{B_0}{|B| + B_0}, \tag{2}$$

where T_c is the critical temperature (=92 K) at $B = 0$ and B_0 (=1.3 T) is constant. The constant value of $\alpha = 4.6 \times 10^8$ A m^{-2} was used for this study, which showed $J_c(40\text{ K}, 0\text{ T}) = 3.3 \times 10^8$ A m^{-2}. Iterative calculation was performed to obtain the convergence of electrical conductivity σ in the bulk at each time step.

The time dependence of the pulsed field $B_{ex}(t)$ along the c-axis with a rise time of τ was approximated as

$$B_{ex}(t) = B_{ex} \frac{t}{\tau} \exp\left(1 - \frac{t}{\tau}\right). \tag{3}$$

The simulation was performed mainly for $\tau = 0.01$ s. It was also performed for $\tau = 0.001$ and 1 s for comparison in section 3.3. The strength of the pulsed field B_{ex} along the c-axis was defined at the position of the bulk centre in the absence of the bulk. Detailed procedures of the simulation and other parameters, including the anisotropic thermal conductivities $\kappa_{ab} = 20$ W m^{-1} K^{-1} in the ab-plane and $\kappa_c = 4$ W m^{-1} K^{-1} along the c-axis, are described elsewhere [13].

3. Results of simulation and discussion

3.1. Trapped field profile and temperature rise

Figures 2(a) and (b) respectively portray the trapped field B_z ($r = 0$) and maximum temperature T_{max} ($r = 0$) at the centre of the bulk surface after applying the pulsed field B_{ex} using the vortex S-coil, vortex L-coil, and the solenoid coil. For the solenoid coil, B_z ($r = 0$) starts to increase at $B_{ex} = 4$ T, becomes a maximum at $B_{ex} = 6$ T and then decreases with a further increase in B_{ex}. The temperature T_{max} ($r = 0$) increased monotonically with increasing B_{ex}. The results of the simulation for the solenoid coil reproduced the experimental ones qualitatively [4]. However, in the case using the vortex S-coil, the magnetic flux starts to be trapped for B_{ex} as low as 1 T and B_z ($r = 0$) increased concomitantly with increasing B_{ex}. The maximum B_z ($r = 0$) was 2.6 T at $B_{ex} = 9$ T, which was higher than that attained using the solenoid coil. The temperature rise for the vortex S-coil increases concomitantly with increasing B_{ex}, but it was about one-third or one-quarter as large as that obtained using the solenoid coil. Figure 2(c) presents experimental results obtained by Ida *et al* for the trapped field B_z on the centre of the GdBaCuO bulk surface at 77 K as a function of applied pulsed field B_{ex} using both the vortex-type coil and the solenoid coil, as re-written from [8].

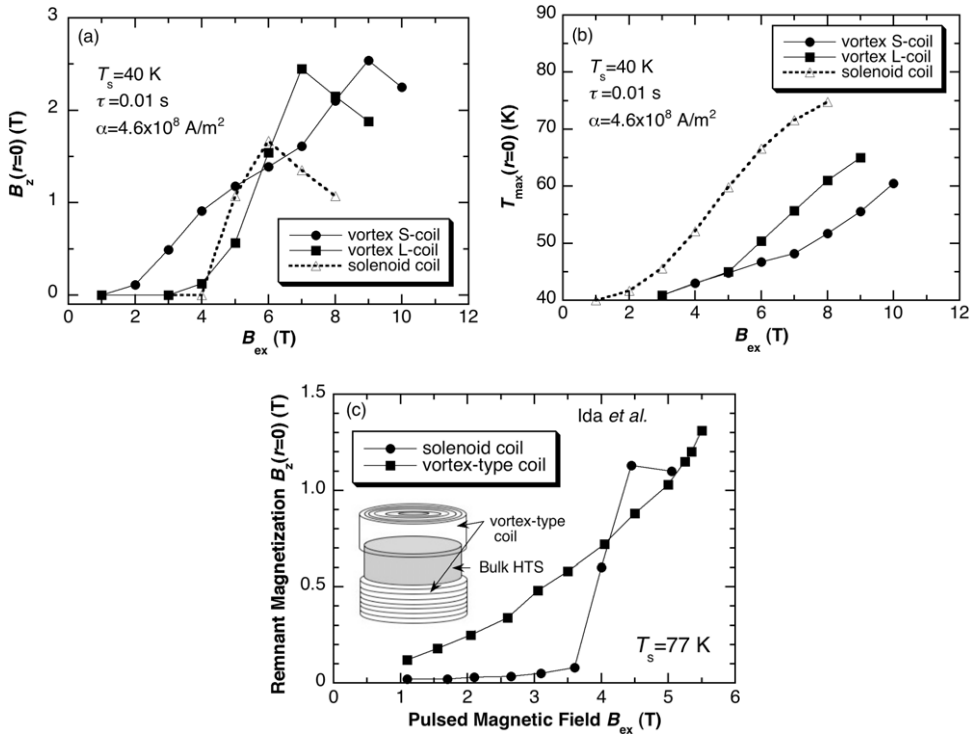

Figure 2. (a) The trapped field B_z ($r = 0$) and (b) the maximum temperature T_{max} ($r = 0$) at the centre of the bulk surface as a function of the applied pulsed field B_{ex} using the vortex S-coil, vortex L-coil, and the solenoid coil. (c) Reported experimental results of remnant magnetization as a function of applied pulsed field using a vortex-type coil and solenoid coil by Ida *et al* [8].

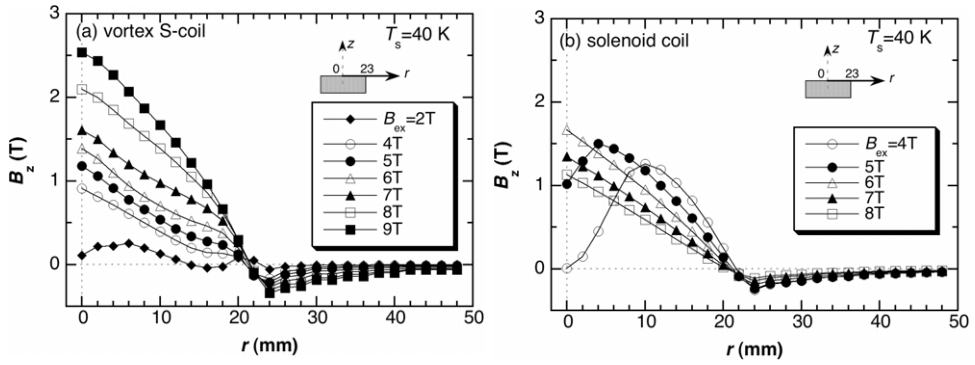

Figure 3. Trapped field $B_z(r)$ profiles on the bulk surface for various applied fields B_{ex} using (a) the vortex S-coil and (b) the solenoid coil.

Comparing with figure 2(a), the results of the simulation qualitatively reproduced the experimental results reported by Ida *et al*.

For the vortex L-coil, B_z ($r = 0$) starts to increase for $B_{ex} \geqslant 4$ T, reaches a maximum at 7 T and then decreases concomitantly with increasing B_{ex}. The B_z ($r = 0$) and T_{max} ($r = 0$) for the vortex L-coil show intermediate behaviours between those of the cases using the vortex S-coil and the solenoid coil. To enhance the B_z value, the OD value should be decreased and then the B_z value using the vortex-type coil is larger than that using the solenoid coil. Hereafter, we focus on the vortex S-coil and compare the characteristics of the trapped field and temperature with those using the solenoid coil.

Figures 3(a) and (b) respectively present the trapped field $B_z(r)$ profiles on the bulk surface for various applied fields B_{ex} using the vortex S-coil and the solenoid coil. The positions of $r = 0$ and 23 mm are, respectively, the centre and edge on the bulk. For the vortex S-coil, the convex $B_z(r)$ profile was achieved even for the lower B_{ex} and $B_z(r)$ increases concomitantly with increasing B_{ex}. The convex shape of the trapped field profile at even lower B_{ex} is advantageous for the realization of the superconducting bulk magnet. However, for the solenoid coil as portrayed in figure 3(b), the $B_z(r)$ profile changes from concave for lower B_{ex} to convex for higher B_{ex}; then the B_z ($r = 0$) value decreases with further increase in B_{ex}. These behaviours using both coils are consistent with experimental results as shown in figure 2(c).

Figure 4 depicts the trapped magnetic flux distribution in the cross section of the bulk after applying the magnetic pulse of $B_{ex} = 4$ and 6 T using the vortex S-coil (left)

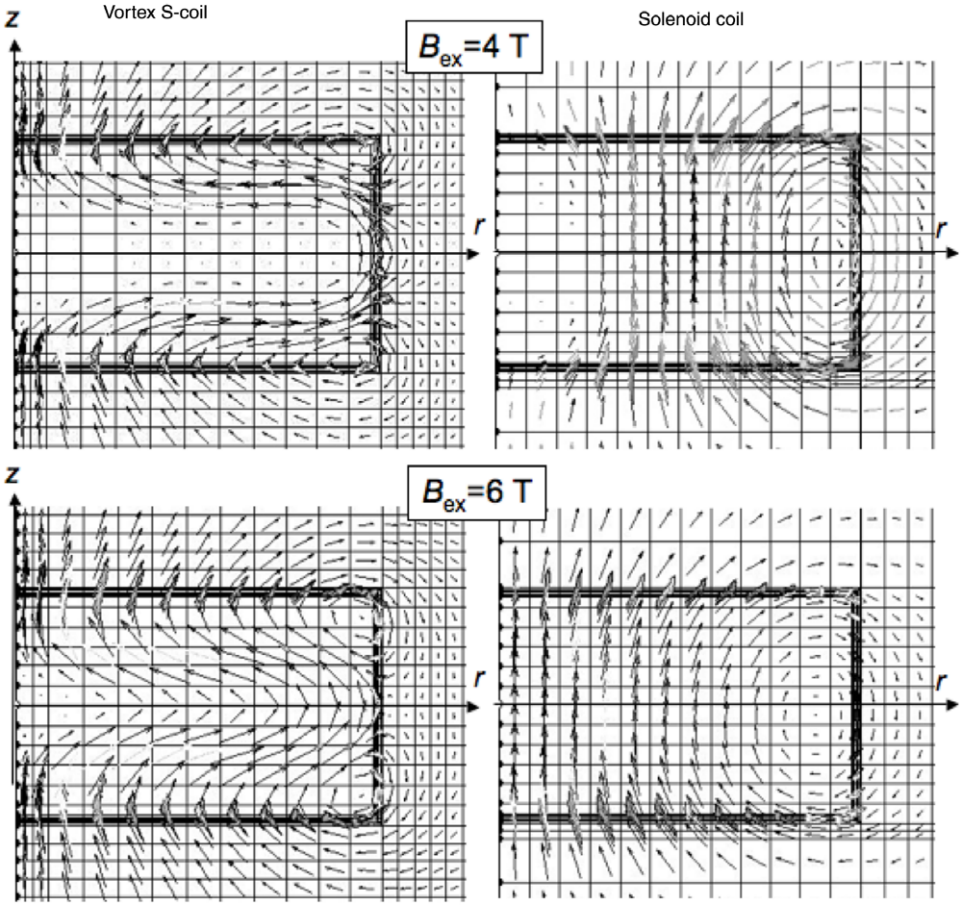

Figure 4. Trapped magnetic flux distribution in the cross section of the bulk after applying the magnetic pulse of $B_{ex} = 4$ and 6 T using the vortex S-coil (left) and the solenoid coil (right).

and the solenoid coil (right). In each panel, arrows indicate the magnitude and the direction of the trapped magnetic field at each position, but the absolute value of the magnitude is arbitrary. For the vortex S-coil, at $B_{ex} = 4$ T, the trapped magnetic flux was oriented towards the r-direction in the inner position and was oriented towards the z-direction on the bulk surface. No flux trap exists in the core of the bulk because of the low B_{ex} value. The magnetic flux starts to intrude into the core of the bulk at $B_{ex} = 6$ T. In addition, the direction of the trapped magnetic field thoroughly aligned to the z-direction with a further increase in B_{ex}. As a result, the trapped field B_z along the z-direction at the centre of the bulk surface increased concomitantly with the increase in B_{ex}.

However, for the solenoid coil, at $B_{ex} = 4$ T, the magnetic flux was trapped mostly around the bulk periphery. No trapped flux exists at the bulk centre. The direction of the trapped field in the bulk was along the z-direction because the magnetic flux intrudes into the bulk from the periphery. The magnetic flux can be trapped at the bulk centre at $B_{ex} = 6$ T and the shape of the trapped field along the z-direction is convex. The magnitude of the magnetic field decreased with a further increase in B_{ex} because of the large temperature rise. In this way, the trapped field profile in the bulk and the magnetizing mechanism differ greatly among magnetizing coils.

3.2. Time dependence of the magnetic flux movement and temperature rise

In section 3.1, the trapped field profile in the bulk differs greatly in the case using each magnetizing coil because of the different mechanism of flux intrusion. In this section, we investigate the time evolution of the flux intrusion and the temperature rise in the bulk using each magnetizing coil. Figures 5(a) and (b) show the time evolution of the local field $B_z(t)$ at $r = 0$, 10, and 20 mm on the bulk surface after applying the magnetic field of $B_{ex} = 6$ T using the vortex S-coil and the solenoid coil, respectively. In the figures, the magnetic pulsed field $B_{ex}(t)$ defined by equation (3) is also shown. Using the vortex S-coil, the local fields $B_z(t)$ at all positions take a maximum around $t = 0.01$ s and then decrease concomitantly with increasing time. The local field B_z ($r = 0$ mm) is the maximum on the bulk surface. However, using the solenoid coil, $B_z(t)$ reaches a maximum at $r = 20$, 10, 0 mm in this order with time and then decreases concomitantly with increasing time.

Figures 6(a) and (b) present the time evolution of the local temperature $T(t)$ at $r = 0$, 10, and 20 mm on the bulk surface after applying the magnetic field of 6 T using the vortex S-coil and the solenoid coil, respectively. Using the vortex S-coil, $T(t)$ at $r = 20$ and 10 mm reach their respective maxima of 50 and 52 K at around $t = 0.01$ s; then they

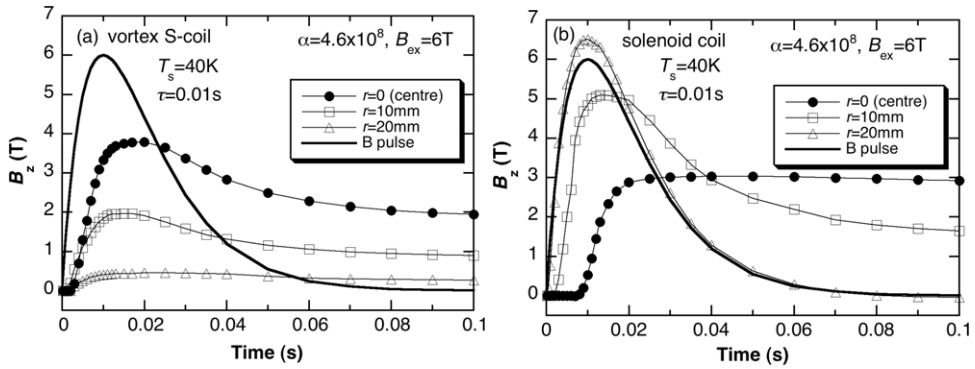

Figure 5. Time evolution of the local field $B_z(t)$ ($r = 0$, 10, and 20 mm) on the bulk surface after applying the magnetic pulse field of $B_{ex} = 6$ T using (a) the vortex S-coil and (b) the solenoid coil. The magnetic pulsed field $B_{ex}(t)$ defined by equation (3) is also shown.

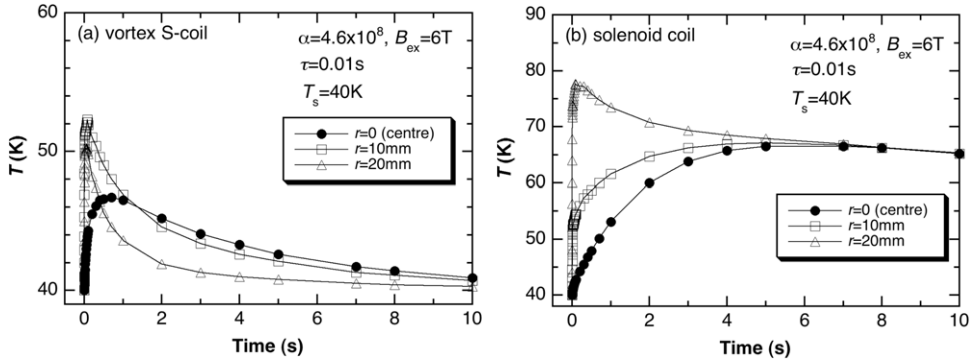

Figure 6. Time evolution of the local temperature $T(t)$ ($r = 0$, 10, and 20 mm) on the bulk surface after applying the magnetic pulse field of 6 T using (a) the vortex S-coil and (b) the solenoid coil.

decrease concomitantly with increasing time. The temperature $T(t)$ at the centre of the bulk surface reaches a maximum of 46.5 K at $t = 0.5$ s and then decreases concomitantly with increasing time. However, using the solenoid coil, $T(t)$ rises and reaches a maximum at $r = 20$, 10, 0 mm in this order with time and then decreases concomitantly with increasing time because of the flux intrusion from the bulk periphery. In those figures, the scales of the ordinates are different. At the centre of the bulk surface ($r = 0$ mm), using the vortex S-coil, the temperature rise is small ($T_{max} = 46.5$ K) and the time t_m at which the temperature rise reaches a maximum is short ($t = 0.5$ s). Using the solenoid coil, the temperature rise is large ($T_{max} = 66$ K) and t_m is 5 s. These results qualitatively reproduce the experimental ones obtained using the solenoid coil and the split coil, which resembles the vortex-type coil [4]. In figures 5 and 6, not only the coil configuration but also the cooling condition differ between the vortex-type coil and the solenoid coil in the results of the simulation. To separate them, an additional simulation was performed for the bulk cooled from the bulk periphery using the solenoid coil.

Figure 7(a) shows the time evolution of the local field $B_z(t)$ at $r = 0$, 10, and 20 mm on the bulk cooled from the bulk periphery after applying the magnetic field of $B_{ex} = 6$ T using the solenoid coil. The coil configuration is illustrated in the inset. Let us compare the results in figure 7(a) and those in figure 5(b). It should be noted that the results in figure 7(a) closely resemble those in figure 5(b) with a slight decrease in $B_z(t)$ at each position because of the difference of the cooling condition. Figures 7(b) and (c) show respectively the trapped field B_z ($r = 0$) and the maximum temperature T_{max} ($r = 0$) for both cooling conditions as a function of the applied field B_{ex}. B_z ($r = 0$) for the bulk cooled from the bulk periphery is slightly larger and T_{max} ($r = 0$) is slightly lower, compared with those for the bulk cooled from the bottom. Because, using the solenoid coil, the heat generation takes place at the bulk periphery mainly and the generated heat was exhausted effectively from the side surface in the bulk cooled from the periphery. As a result, the cooling condition was hardly influenced for the field trap and the differences in the field trap between the vortex-type coil and the solenoid coil, as shown in figure 2(a), result from the coil configuration.

3.3. Effect of the rise time of the magnetic pulse using a vortex-type coil

In a previous paper, we presented a long magnetic pulse application during PFM as a possible solution to enhance the trapped field using the solenoid coil [13]. In this section, we discuss the effect of the rise time elongation of the magnetic pulse on the trapped field characteristics using the vortex S-coil. Figures 8(a) and (b) depict the trapped field B_z ($r = 0$) and maximum temperature T_{max} ($r = 0$) at the centre of the bulk surface as a function of the applied field B_{ex} for various rise times τ of the magnetic pulse. The results for $\tau = 0.01$ s

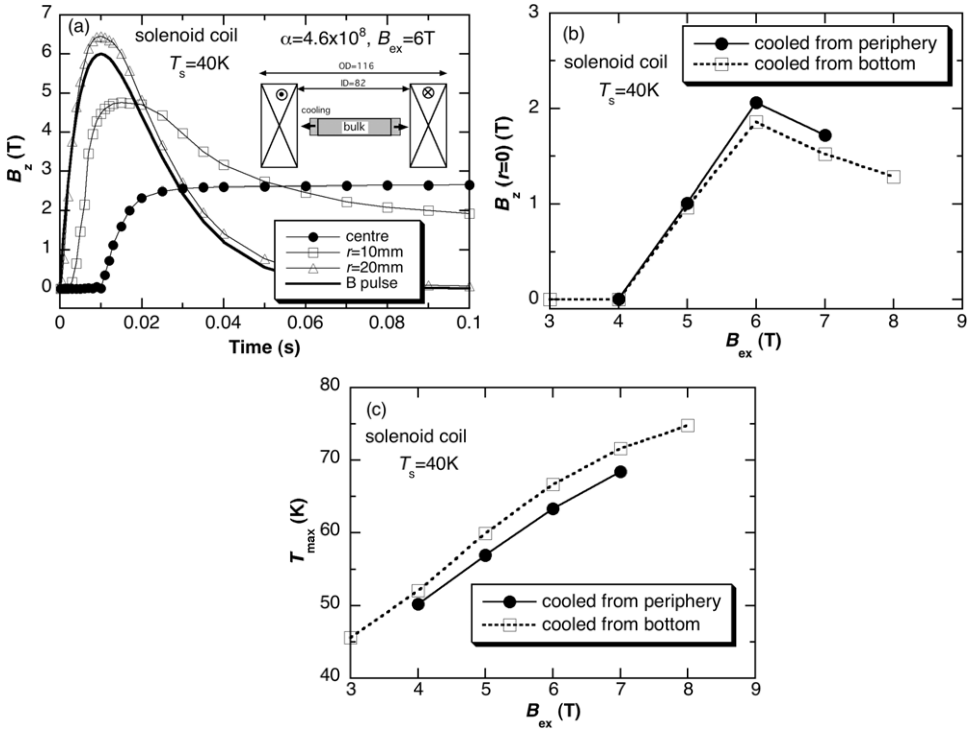

Figure 7. (a) Time evolution of the local field $B_z(t)$ ($r = 0$, 10, and 20 mm) on the bulk cooled from the bulk periphery after applying a magnetic pulse field of 6 T using the solenoid coil. (b) The trapped field B_z ($r = 0$) and (c) the maximum temperature T_{max} ($r = 0$) for both cooling conditions as a function of the applied field B_{ex} (see text).

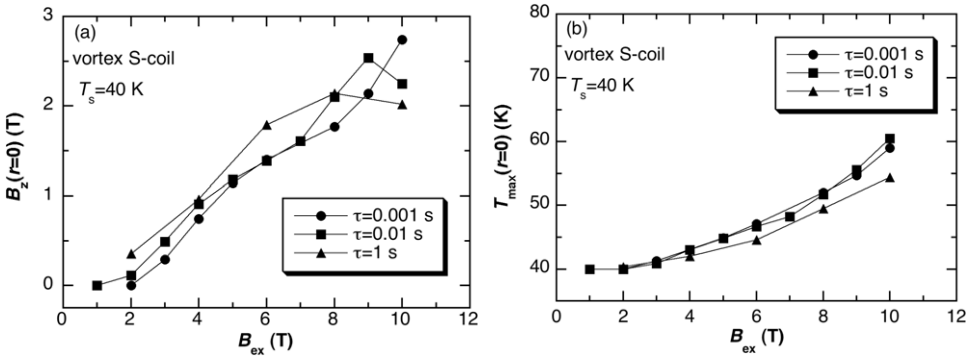

Figure 8. (a) The trapped field B_z ($r = 0$) and (b) the maximum temperature T_{max} ($r = 0$) at the centre of the bulk surface as a function of the applied field B_{ex} for various rise times τ of the magnetic pulse.

are also shown. For $B_{ex} \leqslant 7$ T, B_z ($r = 0$) increases slightly with increasing τ, and for $B_{ex} \geqslant 8$ T, B_z ($r = 0$) decreases slightly with increasing τ. However, it should be noted that no large difference exists for each τ value, which differs greatly from that obtained when using the solenoid coil [13]. These results show that a similar trapped field is obtainable even for small τ values and suggest that the condenser bank capacity used for PFM can be down-sized. In PFM, after a large amount of electricity is charged in the capacitance in the condenser bank, it is discharged through the magnetizing coil. The rise time τ becomes short with the decrease in the inductance L of the coil and capacitance C of the condenser bank. As a result of the short τ value, the volume of the condenser bank can be down-sized, although it is necessary to enhance the charged voltage. The suggestion is quite favourable for practical applications.

4. Summary

Numerical simulations of magnetic flux propagation and the temperature rise were performed for a cryo-cooled superconducting bulk disc using a vortex-type coil after applying a magnetic pulse, compared with those using a conventional solenoid coil. A summary of important results of the simulation and conclusions obtained from this study is presented below.

(1) The applied pulsed field dependence of the trapped field B_z using the vortex-type coil qualitatively reproduced the

experimental results reported by Ida *et al*. The magnetic field can be trapped even for a lower applied pulsed field and the maximum trapped field can be enhanced more than when using a solenoid coil. To enhance the B_z value, the outer diameter (OD) of the vortex-type coil must be less than that of the superconducting bulk disc.

(2) The time and spatial dependence of the local field and temperature in the bulk were simulated, revealing a clear difference in the magnetizing mechanism. For the vortex-type coil, the magnetic flux intrudes mainly into the bulk from the surfaces. However, for the solenoid coil, all magnetic fluxes intrude into the bulk from the periphery.

(3) The temperature rise during the flux intrusion for the vortex S-coil is one-third or one-quarter as large as that for the solenoid coil. Reduction in the maximum temperature rise also enhances the trapped field.

(4) The effect of rise time elongation of the pulsed field on the trapped field enhancement has been simulated: the rise time τ was changed from 0.001 to 1 s. No large differences were found in the trapped field for each τ value. In other words, a similar trapped field is obtainable even for small τ values. These results suggest that the capacity of the condenser bank used in PFM can be down-sized, which is favourable for practical applications. The results of the simulation for the vortex-type coil must be reproduced and verified through further detailed experimentation.

References

[1] Yanagi Y, Itoh Y, Yoshikawa M, Oka T, Hosokawa T, Ishihara H, Ikuta H and Mizutani U 2000 *Advances in Superconductivity XII* (Tokyo: Springer) p 470

[2] Sander M, Sutter U, Koch R and Klaser M 2000 *Supercond. Sci. Technol.* **13** 841

[3] Fujishiro H, Oka T, Yokoyama K, Kaneyama M and Noto K 2004 *IEEE Trans. Appl. Supercond.* **14** 1054

[4] Fujishiro H, Hiyama T, Miura T, Naito T, Nariki S, Sakai N and Hirabayashi I 2009 *IEEE Trans. Appl. Supercond.* **19** 3545

[5] Fujishiro H, Hiyama T, Tateiwa T, Yanagi Y and Oka T 2007 *Physica* C **463–465** 394

[6] Fujishiro H, Kaneyama M, Tateiwa T and Oka T 2003 *Japan. J. Appl. Phys.* **44** L1221

[7] Fujishiro H, Tateiwa T, Fujiwara A, Oka T and Hayashi H 2006 *Physica* C **445–448** 334

[8] Ida T *et al* 2004 *Physica* C **412–414** 638

[9] Yamaguchi K, Kimura Y, Izumi M, Nariki S, Sakai N and Hirabayashi I 2008 *J. Phys.: Conf. Ser.* **97** 012278

[10] Braeck S, Shantsev D V, Johansen T H and Galperin Y M 2002 *J. Appl. Phys.* **92** 6235

[11] Berger K, Leveque J, Netter D, Douine B and Rezzoug A 2007 *IEEE Trans. Appl. Supercond.* **17** 3028

[12] Ohsaki H, Matsumura S, Kawamoto S and Shiraishi R 2008 *AIP Conf. Proc.* **985** 999

[13] Fujishiro H and Naito T 2010 *Supercond. Sci. Technol.* **23** 105021

[14] Fujishiro H, Naito T and Furuta D 2011 *IEEE Trans. Appl. Supercond.* at press

[15] Fujishiro H, Naito T and Oyama M 2011 *Physica* C at press